Journal of ELECTRONIC MATERIALS, Vol. 45, No. 3, 2016
DOI: 10.1007/s11664-015-4003-2

Bonding of Bi_2Te_3-Based Thermoelectric Legs to Metallic Contacts Using $Bi_{0.82}Sb_{0.18}$ Alloy

ROI VIZEL,[1] TAL BARGIG,[1] OFER BEERI,[1,2] and YANIV GELBSTEIN[1,3]

1.—The Department of Materials Engineering, Ben-Gurion University of the Negev, Beer-Sheva, Israel. 2.—e-mail: ofer.beeri@gmail.com. 3.—e-mail: yanivge@bgu.ac.il

Thermoelectrics is gaining increased attention as a renewable direct energy conversion method from heat to electricity. The most efficient and up-to-date thermoelectric materials for temperatures of up to 250°C are $(Bi_{1-x}Sb_x)_2(Te_{1-y}Se_y)_3$ alloys. In the current research, to discover practical thermoelectric power generation devices capable of operation at such temperatures, $Bi_{0.82}Sb_{0.18}$ alloy was considered as a lead-free high-temperature (<250°C) solder composition for bonding of *n*-type $Bi_2Te_{2.4}Se_{0.6}$ and *p*-type $Bi_{0.4}Sb_{1.6}Te_3$ legs into Cu, Ag, Ni and Fe metallic bridges. In the case of Cu, fine contacts with low electrical contact resistance of $\sim 1.5 \pm 0.5$ mΩ mm^2 were observed upon soldering at 350°C.

Key words: Thermoelectrics, Bi_2Te_3, bonding, Bi-Sb

INTRODUCTION

New alternative energy resources enabling new technological developments and bringing society one step closer to a cleaner environment are constantly being investigated. Thermoelectrics (TE) is one of the emerging technologies for direct conversion of waste heat into useful electricity, enabling the reduction of the global reliance on fossil fuels as energy sources and therefore of the reduction of automotive fuel consumption and CO_2 emissions. For temperatures up to ~250°C, Bi_2Te_3-based TE alloys and specifically the *p*-type $Bi_xSb_{2-x}Te_3$[1–7] and *n*-type $Bi_2Te_xSe_{3-x}$[8–11] compositions are known as the most efficient TE materials. Although a large enhancement of the TE figure-of-merit, ZT ($=\alpha^2 T/\rho\kappa$, where α is the Seebeck coefficient, ρ the electrical resistivity, κ the thermal conductivity and T the absolute temperature) of Bi_2Te_3-based materials, is constantly being reported, mainly due to nanostructuring and lattice thermal conductivity reduction,[1] no practical TE devices with enhanced efficiency, capable of serving as TE generators at temperatures of up to 250°C, have been reported to date. A possible reason for this can be attributed to insufficient couples' bonding techniques, resulting so far in high-contact resistances and mechanical instability. Regardless of the great importance of TE couples development for increasing the technology readiness level toward efficient TE devices, only very limited data have been so far reported in this field. Cu,[12–14] Ni[15] and Ag[14,16] bridges have been mostly explored as metallic contacts in Bi_2Te_3 couples. The eutectic Sn-37Pb alloy, which has been widely applied in micro-electronics applications, exhibits a very low melting temperature of ~183°C,[17] which might only be useful for low-temperature (e.g. cooling) TE applications, in addition to the fact that it contains the not environmentally friendly Pb element. Among the more modern Pb-free solder alloys, Sn-3.5Ag, Sn-3Ag-0.5Cu and Sn-0.7Cu have been successfully applied for bonding of Bi_2Te_3-based legs to both Ag and Cu contacts;[14] however, the melting points of these compositions are around ~220°C,[17] which are still low for fulfilling the potential of Bi_2Te_3-based TE power generators. Due to the fact that the low melting temperatures of the currently applied Sn-based solder materials originate from the low melting temperature of pure Sn (~232°C), the current research was focused on Pb-free Sb (melting temperature of ~631°C)-based solder materials and specifically on $Bi_{1-x}Sb_x$ alloys. In the Bi-Sb binary

(Received May 27, 2015; accepted August 18, 2015; published online October 29, 2015)

system, a complete miscibility between Bi and Sb exists, with solidus temperatures (onset of melting) higher than ~300°C and melting (liquidus) temperatures higher than ~ 350°C, for x values higher than 0.18.[18] Due to an expected higher chemical compatibility to Bi_2Te_3-based TE legs with increasing the Bi content of the solder materials, in addition to the requirement to reduce the liquidus temperature as much as possible to avoid melting the TE elements during the soldering process, the research was focused on the $Bi_{0.82}Sb_{0.18}$ alloy. Bi-rich $Bi_{1-x}Sb_x$ alloys have been widely investigated as n-type semiconducting TE compositions for cooling applications at temperatures around or lower than room temperature,[19–21] but as far as we know have never been considered before as solder compositions. In the current research, bonding experiments between the previously reported n-type 0.1% CHI_3-doped $Bi_2Te_{2.4}Se_{0.6}$[22] and p-type $Bi_{0.4}Sb_{1.6}Te_3$[23] compositions to Fe, Ni, Ag and Cu metallic bridges, with the aid of the $Bi_{0.82}Sb_{0.18}$ solder alloy, were investigated, as the first step for developing of TE Bi_2Te_3-based power generation devices capable of operating at temperatures up to ~250°C. We show that, although the $Bi_{0.82}Sb_{0.18}$ solder alloy exhibits n-type semiconducting properties following arc-melting synthesis, it reacts with all the investigated metallic (i.e. Fe, Ni, Ag and Cu) bridges, to form a Bi-rich contact layer surrounded by Sb-based phases. The nature of the various involved phases is discussed in detail. TE couples based on the above-mentioned n- and p-type Bi_2Te_3-based TE legs bonded into Cu metallic bridges exhibited very low contact resistance of $\sim 1.5 \pm 0.5$ mΩ mm^2 which is within the required range for TE practical power generation devices.[24]

EXPERIMENTAL

n-type 0.1 wt.% CHI_3-doped $Bi_2Te_{2.4}Se_{0.6}$ and p-type $Bi_{0.4}Sb_{1.6}Te_3$ ingots were synthesized from pure Bi, Te, Se, Sb and CHI_3 constituents in vacuum (10^{-5} Torr)-sealed quartz ampoules, at 850°C for 1.5 h, using a rocking split tube furnace (Thermcraft, USA). The ingots were crushed to a maximal powder size of 250 μm using an agate mortar and pestle, cold-pressed at a mechanical pressure of 800 MPa and sintered under an inert argon atmosphere at 400°C for 10 h. Following sintering, the samples' densities were found to be higher than 95% of the theoretic values. $Bi_{0.82}Sb_{0.18}$ alloy, as a soldering composition, was synthesized by arc-melting (MAM-1; Edmund Bühler, Germany) from pure elements, under argon atmosphere, with more than five flipping and re-melting stages to ensure homogeneity. The crystal structure was analyzed by x-ray diffraction (XRD; Rigaku DMAX 2100 powder diffractometer) to ensure a single phase composition for each of the synthesized alloys. The microstructural characterizations and the chemical composition analyses were conducted by scanning electron microscopy (SEM; JEOL JSM-5600) and energy-dispersive x-ray spectroscopy (EDS), respectively. α and ρ were measured by a Linseis LSR-3/800 Seebeck coefficient/electrical resistance measuring system. κ was determined by using the flash diffusivity method (LFA 457; Netzsch). All the transport properties were measured transverse to the pressing direction. The melting temperature of the solder alloy was analyzed using a differential scanning calorimetry (STA 449; Netzsch). Two identical pure Fe, Ni, Ag and Cu metallic plates ($2 \times 8 \times 18$ mm^3) of each type, following ultrasonic cleaning in acetone, were soldered to each other by the $Bi_{0.82}Sb_{0.18}$ solder alloy, at 450°C for 30 min under argon atmosphere, in order to investigate the chemical compatibility and solderability to these metallic plates. Soldering the n-type 0.1 wt.% CHI_3-doped $Bi_2Te_{2.4}Se_{0.6}$ and p-type $Bi_{0.4}Sb_{1.6}Te_3$ TE legs, each with a diameter of 6 mm and length of 12 mm and at temperatures of 350°C and 450°C, into Cu metallic plates to form TE couples under similar conditions was also performed. The soldering process included grinding the $Bi_{0.82}Sb_{0.18}$ solder alloy into 0.2 g powder, which was applied at the junction between the TE legs and the Cu bridge. The entire array of TE legs, solder powder and metallic bridge was placed in a graphite die and was pressed together under a 3-kg weight applied evenly to each of the legs.

The contact resistance was measured by a four-point probe in a procedure described previously,[24] based on measuring the electrical resistance of each of the TE legs (n and p) prior to the bonding. Following bonding, the total electrical resistance of the individual legs and the contacts to the adjacent metallic plates was measured, while the the contact resistance was calculated by subtraction of the original leg's resistance from the total measured values.

RESULTS AND DISCUSSION

Following synthesis, both the p- and n-TE legs' compositions and the solder alloy exhibited the expected single phase $Bi_{0.4}Sb_{1.6}Te_3$, $Bi_2Te_{2.4}Se_{0.6}$ $Bi_{0.82}Sb_{0.18}$ compositions, respectively, by XRD and SEM analyses. Differential scanning calorimetry (DSC) for the $Bi_{0.82}Sb_{0.18}$ solder alloy up to 500°C indicated two endothermic peaks at ~300°C and ~340°C (Fig. 1a, points 1 and 2, respectively), reflecting an onset of melting by crossing the solidus curve into a solid–liquid two-phase zone, and a final melting by crossing the liquidus curve, respectively, in agreement with the temperatures associated with this composition in the Bi-Sb binary phase diagram[18] (Fig. 1b). From the phase diagram shown in Fig. 1b, it can be clearly understood that the currently investigated $Bi_{0.82}Sb_{0.18}$ solder composition was chosen as one exhibiting a solidus temperature (point 1) slightly higher than the maximal practical operation temperature of Bi_2Te_3-based TE couples

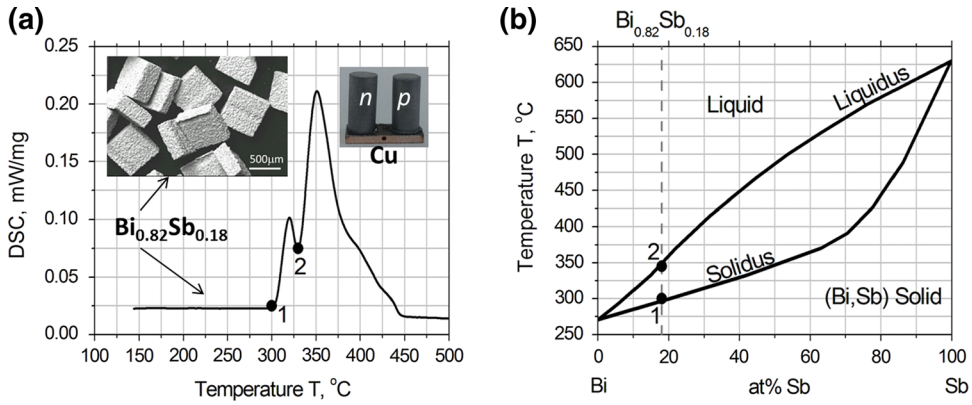

Fig. 1. (a) Differential scanning calorimetry results of the $Bi_{0.82}Sb_{0.18}$ solder alloy. The insets indicate a SEM macroscopic view of the $Bi_{0.82}Sb_{0.18}$ sliced plates and a TE couple soldered into a Cu metallic bridge. (b) Bi-Sb binary phase diagram[18] indicating the onset (*1*) and the finish (*2*) melting temperatures for the currently investigated $Bi_{0.82}Sb_{0.18}$ composition.

(~250°C) with the minimal liquidus temperature (point 2) for avoiding deterioration of the TE legs during the soldering process, due to sublimation of tellurium and/or any possible eutectic with the metallic bridges.

The temperature dependence of the TE transport properties of the investigated $Bi_{0.82}Sb_{0.18}$ solder, *p*-type $Bi_{0.4}Sb_{1.6}Te_3$ and *n*-type $Bi_2Te_{2.4}Se_{0.6}$ alloys, α, ρ, κ and *ZT*, following the synthesis are shown in Fig. 2a–d, respectively. It can be clearly seen in Fig. 2a that, as expected, the $Bi_{0.4}Sb_{1.6}Te_3$ and $Bi_2Te_{2.4}Se_{0.6}$ TE alloys exhibit positive and negative α values, respectively, indicating their *p*- and *n*-type conduction nature, respectively, while the $Bi_{0.82}Sb_{0.18}$ solder alloy exhibits a weak *n*-type semiconducting nature, indicated by the negative α with low absolute values, approaching those of metallic alloys.

The more metallic nature (higher carrier concentration) of the $Bi_{0.82}Sb_{0.18}$ solder alloy compared to the investigated *n*- and *p*-TE elements can also be observed by the lower ρ (Fig. 2b) and higher κ (Fig. 2c) values of this composition, highlighting its potential to serve as a contact material with low electrical and thermal contact resistance in TE devices. Regarding *ZT*, it can be clearly seen in Fig. 2d that much lower values were obtained for the $Bi_{0.82}Sb_{0.18}$ alloy compared to the other *n*- and *p*-type compositions, indicating that this composition is much less TE efficient in the entire investigated temperature range. This fact can also be attributed to the higher metallic nature of $Bi_{0.82}Sb_{0.18}$, associated with much higher carrier concentration than the optimal for TE applications. On the other hand, the increasing trend of *ZT* for $Bi_{0.82}Sb_{0.18}$ with decreasing the temperature is in agreement with the above-reported application of $Bi_{1-x}Sb_x$ alloys in TE cooling at temperatures below room temperature.

SEM micrographs following $Bi_{0.82}Sb_{0.18}$ soldering of similar Ag, Cu, Fe and Ni plates to each other at 450°C are shown in Fig. 3a–d.

In these micrographs, it can be clearly seen that both Ag (Fig. 3a) and Cu (Fig. 3b) react similarly with the $Bi_{0.82}Sb_{0.18}$ solder. In both these cases, Sb from the solder diffuses into the metallic plate, while enriching the Bi concentration of the original $Bi_{0.82}Sb_{0.18}$ contact. This diffusion into the metallic plates resulted for the Ag case in Ag metal enriched by Sb (Fig. 3a), and, for the Cu case, the formation of the Cu-rich $Cu_{0.75}Sb_{0.25}$ phase and others inside the Cu plate (Fig. 3b). This trend is in contrast to that observed for the Fe (Fig. 3c) and Ni (Fig. 3d) cases, in which both Fe and Ni diffuse into the solder, while reacting with the $Bi_{0.82}Sb_{0.18}$ layer for the formation of Sb-rich phases (i.e. $FeSb_2$ and $Fe_{1.27}Sb$ for the case of Fe, Fig. 3c, and NiSb for the case of Ni, Fig. 3d). This behavior is in agreement with the much higher diffusion coefficients of Sb in Cu and Ag[25–27] and the previously reported binary Cu-Sb[28] and Ag-Sb[29] phase diagrams, indicating the existence of only Cu- and Ag-rich compounds and no Sb-rich compounds at all, motivating a diffusion of Sb from the solder toward the metal-rich metallic plates for the formation of these phases. On the other hand, in the Ni-Sb[30] and Fe-Sb[31] binary phase diagrams, Sb-rich compounds also exist, motivating an inverse diffusion of the metals from the metallic plates to diffuse into the Sb-richer solder for their formation. Due to the fact that inter-metallic compounds usually exhibit a mechanically brittle nature, their formation inside the metallic bridges of the TE couples, which are subjected to high shear stresses during the operation, is not favorable. On the other hand, the brittleness of scattered inter-metallic compounds inside the original $Bi_{0.82}Sb_{0.18}$ contact layer might be compensated by the solder's soft and ductile nature. A final decision on the preference of one mechanism on the other, if any, for enhancing TE couples' durability requires further analyses including mechanical properties and finite elements modeling approaches that were not taken at this stage of the research. Yet, regardless which of the mechanisms is more preferable, TE couples,

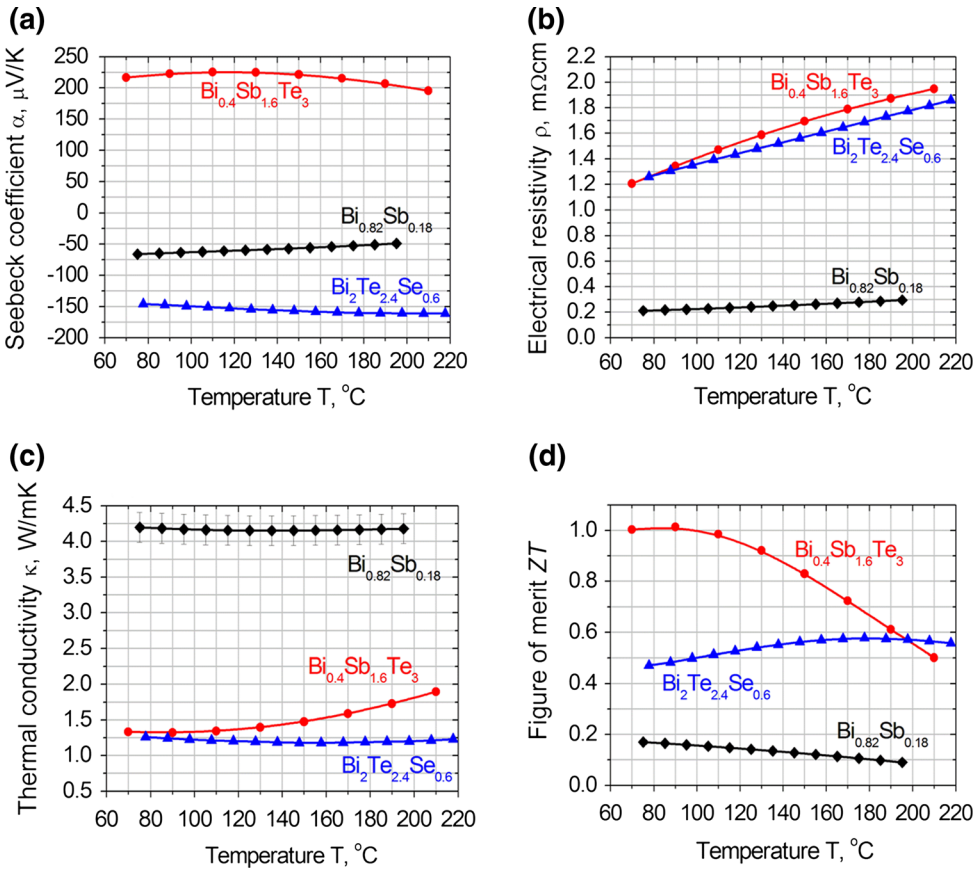

Fig. 2. Temperature dependence of the TE transport properties of the investigated $Bi_{0.82}Sb_{0.18}$ solder, *p*-type $Bi_{0.4}Sb_{1.6}Te_3$ and *n*-type $Bi_2Te_{2.4}Se_{0.6}$ alloys, (a) Seebeck coefficient, α, (b) electrical resistivity, ρ, (c) thermal conductivities, κ, and the (d) TE figure-of-merit, *ZT*.

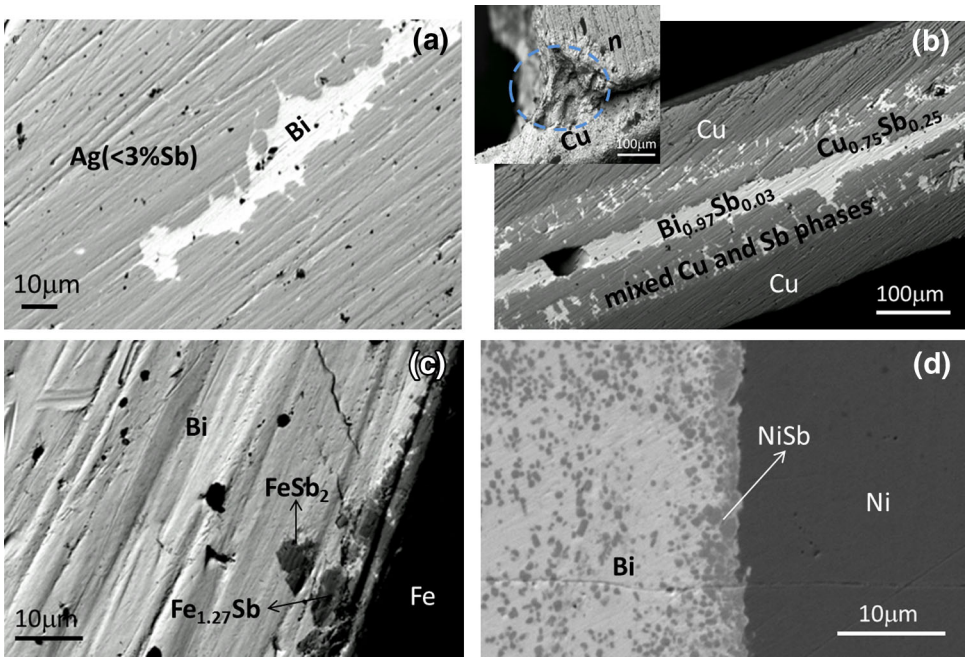

Fig. 3. SEM micrographs following $Bi_{0.82}Sb_{0.18}$ soldering of similar Ag (a), Cu (b), Fe (c) and Ni (d) plates to each other at 450°C. The inset in (b) shows a strong interaction zone and partial melting of the leg in the vicinity of contact between the *n*-$Bi_2Te_{2.4}Se_{0.6}$ leg and the Cu metallic bridge following soldering at 450°C.

based on the investigated *n*- and *p*-legs, were $Bi_{0.82}Sb_{0.18}$ soldered to Cu plates at the same 450°C temperature. At this temperature, a strong reaction zone was observed in the contact with the TE legs and the Cu metallic bridge (an example is shown in the inset of Fig. 3b), due to possible eutectic and/or sublimation of Te, implying that 450°C is too high for the investigated TE legs' composition. An enhanced Te sublimation at a soldering temperature of 450°C, together with the formation of Sb-rich phases, might enrich the Bi concentration of the *n*- and *p*-type TE legs and the solder material, leading at local points to nearly pure Bi phase in the vicinity of the contact, having a melting temperature of ≤300°C. Reduction of the soldering temperature to 350°C resulted in fine couples (see the righthand inset of Fig. 1a), with contact resistance of 1.5 ± 0.5 mΩ mm^2, which is within the range required for practical TE power generation devices.[24,32]

CONCLUSIONS

In the current research, the $Bi_{0.82}Sb_{0.18}$ alloy, was investigated as a solder composition for TE power generation of $(Bi_{1-x}Sb_x)_2(Te_{1-y}Se_y)_3$-based devices by being subjected to operating temperatures of up to 250°C. Fine contacts upon soldering of two similar Ag, Fe, Cu and Ni metallic plates at 450°C were observed. Yet, two different metallurgical mechanisms were identified by SEM during the bonding operation. For the Ag and Cu cases, Sb diffusion outside the bonding area toward the metallic plates was identified, while, for the cases of Fe and Ni, atoms from the metallic plates were diffused into the bonding area for the formation of Sb-rich phases. TE couples' soldering at the same temperatures, using Cu metallic plates, resulted in strong interaction zones in the vicinity of the contact between the metallic bridges and the $(Bi_{1-x}Sb_x)_2(Te_{1-y}Se_y)_3$ alloys, which were attributed to possible eutectic and/or sublimation of Te, implying that 450°C is too high for practical soldering. Reduction of the soldering temperature to 350°C resulted in fine couples with contact resistance of 1.5 ± 0.5 mΩ mm^2, which is within the range required for practical TE power generation devices.

ACKNOWLEDGEMENTS

The authors would like to thank MAFAT (contract No. 4440585588, 2014) and the Israeli Ministry of Science, Technology and Space (Oil substitutions for transportation grant, 2014) for supporting this research and to Mr. Yair George for the synthesis of the alloys and specimen preparation.

REFERENCES

1. W. Xie, X. Tang, Y. Yan, Q. Zhang, and T.M. Tritt, *Appl. Phys. Lett.* 94, 102111 (2009).
2. C. Drasar, A. Hovorkova, P. Lostak, S. Ballikaya, C.-P. Li, and C. Uher, *J. Electron. Mater.* 39, 1760 (2010).
3. B. Poudel, Q. Hao, Y. Ma, Y. Lan, A. Minnich, Yu Bo, X. Yan, D. Wang, A. Muto, D. Vashaee, X. Chen, J. Liu, M.S. Dresselhaus, G. Chen, and Z. Ren, *Science* 320, 634 (2008).
4. D. Vasilevskiy, M.S. Dawood, J.-P. Masse, S. Turenne, and R.A. Masut, *J. Electron. Mater.* 39, 1890 (2010).
5. R.J. Schwartz, *J. Appl. Phys.* 38, 2865 (1967).
6. A. Kadhim, A. Hmood, and H.A. Hassan, *J. Electron. Mater.* 42, 1017 (2013).
7. N. Bomshtein, G. Spiridonov, Z. Dashevsky, and Y. Gelbstien, *J. Electron. Mater.* 41, 1546 (2012).
8. J.J. Shen, L.P. Hu, T.J. Zhu, and X.B. Zhao, *Appl. Phys. Lett.* 99, 124102 (2011).
9. N. Gothard, X. Ji, J. He, and T.M. Tritt, *J. Appl. Phys.* 103, 054314 (2008).
10. X. Yan, B. Poudel, Y. Ma, W.S. Liu, G. Joshi, H. Wang, Y. Lan, D. Wang, G. Chen, and Z.F. Ren, *Nano Lett.* 10, 3373 (2010).
11. W.-S. Liu, Q. Zhang, Y. Lan, S. Chen, X. Yan, Q. Zhang, H. Wang, D. Wang, G. Chen, and Z. Ren, *Adv. Energy Mater.* 1, 577 (2011).
12. C.-N. Liao, W.-T. Chen, and C.-H. Lee, *Appl. Phys. Lett.* 97, 241906 (2010).
13. H.-H. Hsu, C.-H. Cheng, Y.-L. Lin, S.-H. Chiou, C.-H. Huang, and C.-P. Cheng, *Appl. Phys. Lett.* 103, 053902 (2013).
14. T.U. Lin, C.N. Liao, and A.T. Wu, *J. Electron. Mater.* 41, 153 (2012).
15. O.D. Iyore, T.H. Lee, R.P. Gupta, J.B. White, H.N. Alshareef, M.J. Kim, and B.E. Gnade, *Surf. Interface Anal.* 41, 440 (2009).
16. W.P. Lin, D.E. Wesolowski, and C.C. Lee, *J. Mater. Sci.* 22, 1313 (2011).
17. T. Siewert, S. Liu, D.R. Smith, and J.C. Madeni, *Database for Solder Properties with Emphasis on New Lead-Free Solders* (Colorado: National Institute of Standards and Technology and Colorado School of Mines, 2002).
18. Y. Feutelais, G. Morgant, J.R. Didry, and J. Schnitter, *Coupling Phase Diagr. Thermochem.* 16, 111 (1992).
19. S. Cho, A. DiVenree, G.K. Wong, and J.B. Ketterson, *J. Appl. Phys.* 85, 3655 (1999).
20. H.J. Liu, L.F. Li, and D. Shi, *J. Electron. Mater.* 35, L7 (2006).
21. T. Luo, S. Wang, H. Li, and X. Tang, *Intermetallics* 32, 96 (2013).
22. T. Shalev, O. Meroz, O. Beeri, and Y. Gelbstein, *J. Electron. Mater.* 44, 1402 (2015).
23. O. Ben-Yehuda, Y. Gelbstein, Z. Dashevsky, R. Shuker, and M.P. Dariel, *J. Appl. Phys.* 101, 113707 (2007).
24. E. Hazan, O. Ben-Yehuda, N. Madar, and Y. Gelbstein, *Adv. Energy Mater.* (2015).
25. H. Giordano, O. Alem, and B. Aufray, *Scr. Metall. Mater.* 28, 257 (1993).
26. E. Sonder, L. Slifkin, and T. Tomizuka, *Phys. Rev.* 93, 970 (1954).
27. S.M. Myers and H.J. Rack, *J. Appl. Phys.* 49, 3246 (1978).
28. X.J. Liu, C.P. Wang, I. Ohnuma, R. Kainuma, and K. Ishida, *J. Phase Equilib.* 21, 432 (2000).
29. E. Zoro, C. Servant, and B. Legendre, *J. Phase Equilib. Diffus.* 28, 250 (2007).
30. Y. Zhang, C. Li, Z. Du, and C. Guo, *CALPHAD* 32, 378 (2008).
31. D. Boa, S. Hassam, G. Kra, K.P. Kotchi, and J. Rogez, *CALPHAD* 32, 227 (2008).
32. W. Liu, H. Wang, L. Wang, X. Wang, G. Joshi, G. Chen, and Z. Ren, *J. Mater. Chem. A* 1, 13093 (2013).